Viscous Friction of Hydrogen-Bonded Matter

Aykut Erbaş,[†,§] Dominik Horinek,[‡] and Roland R. Netz*[,†,§]

[†]Physik Department, Technische Universität München, 85748 Garching, Germany,

[‡]Institut für Physikalische und Theoretische Chemie, Universität Regensburg, 93040 Regensburg, Germany

[§]Fachbereich Physik, Freie Universität Berlin, 14195 Berlin, Germany

S *Supporting Information*

ABSTRACT: Amontons' law successfully describes friction between macroscopic solid bodies for a wide range of velocities and normal forces. For the diffusion and forced sliding of adhering or entangled macromolecules, proteins, and biological complexes, temperature effects are invariably important, and a similarly successful friction law at biological length and velocity scales is missing. Hydrogen bonds (HBs) are key to the specific binding of biomatter. Here we show that friction between hydrogen-bonded matter obeys in the biologically relevant low-velocity viscous regime a simple law: the friction force is

proportional to the number of HBs, the sliding velocity, and a friction coefficient γ_{HB}. This law is deduced from atomistic molecular dynamics simulations for short peptide chains that are laterally pulled over planar hydroxylated substrates in the presence of water and holds for widely different peptides, surface polarities, and applied normal forces. The value of γ_{HB} is extrapolated from simulations at sliding velocities in the range from $V = 10^{-2}$ to 100 m/s by mapping on a simple stochastic model and turns out to be of the order of $\gamma_{HB} \simeq 10^{-8}$ kg/s. The friction of a single HB thus amounts to the Stokes friction of a sphere with an equivalent radius of roughly 1 μm moving in water. Cooperativity is pronounced: roughly three HBs act collectively.
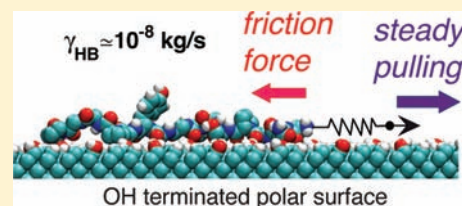
INTRODUCTION

Hydrogen bonds (HBs), with their unique combination of short-range and pronounced directionality, are optimally suited for the controlled assembly of macromolecular complexes and devices. They have been used to design self-healing polymeric adhesives[1] as well as polymer networks with tailored material properties.[2,3] HBs are responsible for the structure of proteins and nucleic acids. Their moderate binding strength of the order of thermal energy allows them to be rearranged one-by-one by biologically available forces. However, when many HBs are probed in parallel, they can withstand large forces and give long-term durability, as has been demonstrated experimentally,[4] in simulations,[5−7] and theoretically.[8] The strength of an adhesive junction is determined not only by the binding constant (i.e., the equilibrium adhesive free energy) but also by the kinetics characterizing the unbinding pathway. Kramer's theory predicts the rate of a reaction as the product of an exponential Arrhenius factor, which contains the activation free energy, and a prefactor. For the reaction between two molecules, this prefactor measures the attempt frequency and is a well-defined quantity. For more complex reactions involving macromolecular binding or conformational change, this prefactor is less well defined. For proteins, it determines the so-called speed limit for folding in the absence of free-energetic barriers[9,10] and takes the form of a diffusion constant (or inverse friction coefficient) along the reaction coordinate.[11,12] The concept of friction historically comes from dry friction between macroscopic solid bodies, where adhesion and temperature effects are irrelevant,[13,14] and is concisely

summarized in terms of Amontons' law, stating that friction force is proportional to normal load but independent of apparent contact area and sliding velocity. In the presence of adhesive contacts and for low sliding velocities, the crossover to viscous friction, where friction force becomes proportional to sliding velocity, is described by Schallamach's phenomenological model,[14,15] which treats the stochastic breakage and rebinding of individual adhesive bonds. Recent single-molecule studies started to bridge the considerable conceptual gap between models for the friction between adhesive macroscopic bodies and the way friction is invoked in protein folding studies: The diffusivity of single DNA molecules adsorbed on cationic bilayers or mica surfaces has been determined using video microscopy,[16,17] from which the friction coefficient can be inferred using Einstein's relation. The velocity-dependent friction of adsorbed polymers has been probed in single-molecule atomic force microscopy studies by pulling single molecules over substrates.[18] Other scenarios where single-molecule friction could be determined are forced slippage between complementary DNA strands[19] and the driven motion of kinesin on microtubules.[20] Some insight into single-molecule friction was provided by molecular dynamics (MD) simulations of adsorbed peptides on surfaces: while adhesive free energies on hydrophobic and hydrophilic surfaces are roughly equal and amount to a few $k_B T$ per residue, the surface friction coefficients are wildly different.[21,22] In fact, the mobility of a

peptide adsorbed on an unpolar surface was similar to that in bulk water. The peptide mobility on a polar surface, however, was orders of magnitude lower and in fact could not be resolved in those simulations due to equilibration issues. We tentatively concluded that hydrophobically collapsed polymers should anneal rather quickly, while a macromolecular collapse driven by intramolecular HBs should be kinetically hampered, in line with experimental findings.[10] We hasten to add that the equilibration of HBs is a universal bottleneck for biomolecular MD simulations in explicit solvent[5,7] and not restricted to any particular model system. A pronounced dependence of the rotational diffusion of solutes[23] and the friction between surfaces[24,25] on the capability to form HBs was experimentally seen, though the interpretation of mesoscopic experiments is complicated because effects due to changes in the number of HBs, the cooperativity between HBs, and the friction contribution from a single HB are difficult to disentangle. While purely hydrophobic surfaces are rare in biology because they would immediately collapse or be covered by adsorbants, polar surfaces are ubiquitous. Understanding the friction of hydrogen-bonded matter at the single-molecule level is clearly important by itself, but it also sheds light on the viscous kinetics of protein folding, ligand−receptor binding, and selective transport in complex biological media. We therefore re-address the issue of peptide friction on polar surfaces, armed with enlarged computer power that allows to simulate peptide sliding at prescribed velocities over 4 orders of magnitude down to $v = 10^{-2}$ m/s and using stochastic theory to extrapolate simulation data into the experimentally important viscous (i.e., linear) friction regime at even lower velocities. As our main result, we find the friction force F_f at low velocities to be proportional to the sliding velocity V and the number of peptide−surface HBs N_{HB}: $F_f = \gamma_{HB} N_{HB} V$. The friction coefficient per HB turns out to be $\gamma_{HB} \simeq 10^{-8}$ kg/s for a wide class of different oligo-peptides, surfaces with different hydroxyl (OH) group coverage and the whole range of studied normal forces. It corresponds to the Stokes friction of a sphere with an equivalent radius of 1 μm moving in water, which vividly demonstrates the pronounced friction provided by HBs. We estimate the cooperativity of our setup to correspond to be $m \simeq 3$ HBs, i.e., units of three HBs act in unison, similar to recent results for the rupturing of HB assemblies.[6] The cooperativity factor m, and thus the friction coefficient γ_{HB}, determined here for a flexible peptide sliding over a hard surface, likely depends on the sliding geometry and in particular on the stiffness of the HB matrix, but it serves as a first guideline for the important case of intraprotein peptide diffusion when HBs are continuously broken and re-formed.

■ METHODS

MD simulations are performed with the Gromacs MD package[26] using the Gromos96 force field[27] and the single point charge (SPC) water model[28] with a constant surface area A, constant vertical pressure $P_z = 1$ bar, and constant temperature $T = 300$ K. For temperature and pressure control, Berendsen's method[29] is used. Periodic boundary conditions for Coulombic interactions are implemented by the Particle-Mesh Ewald method.[30] For the nonpolar surface, a (100) elastic diamond substrate is saturated completely by uncharged hydrogen atoms. For the polar surface, a varying fraction Φ of the H atoms are replaced by OH groups which are distributed on a regular square lattice on the diamond surface and are able to rotate. For the partial charges of COH, the values of a serine residue are used: $q_C = 0.266$ e, $q_O = -0.674$ e, and $q_H = 0.408$ e. We consider different homopeptides as well as one heterogeneous spider silk peptide. For

the spider silk 15-mer we use the sequence NQGPSGPGGYGPGGP, which corresponds to the terminal fragment of the mildly hydrophobic C_{16} ADF-4 silk protein which was extensively studied experimentally and theoretically,[21,22] where N, Q, G, P, S, and Y denote asparagine, glutamine, glycine, proline, serine, and tyrosine amino acids, respectively. As homogeneous peptides we study glycine, hydrophilic asparagine, and hydrophobic leucine chains with $N = 6-22$ residues. Although spider silk peptides are in principle more complex than homopeptides due to specific sequence effects, they are convenient for experimental as well as theoretical studies because they are easily solvable in water and at the same time show only weak structuring due to a subtle balance of hydrophobic and hydrogen-bonding effects. In most of our simulations, a harmonic spring is connected to the peptide terminus and moved at constant velocity V laterally over the surface. The spring exerts no vertical force, and the spring constant is chosen between $k = 3$ and 1350 pN/nm such that the spring extension is roughly half the simulation box size. Typical lateral dimensions of the diamond surfaces are 6 nm × 3 nm, and the diamond thickness is 1.8 nm. Typically 3000 water molecules are simulated, giving a total simulation box height of at least 5 nm. For the longest peptide chains the lateral system size is increased. Simulation runs up to 1 μs are performed with an integration time step of 2 fs. Peptides are allowed to adsorb and equilibrate on the surface prior to lateral pulling. Error bars are calculated via block averaging and shown only when larger than the symbol size. Further checks on finite size, finite peptide length, and diamond elasticity effects and comparison of terminally and homogeneously pulled peptides are presented in the Supporting Information (SI). When counting HBs, the acceptor−hydrogen−donor angle θ should be smaller than $\theta = 30°$ and the donor−acceptor distance smaller than $d = 0.35$ nm.[31] More details on simulations are given in the SI.

■ RESULTS AND DISCUSSION

Lateral Pulling of Peptides on Polar and Unpolar Surfaces. In our simulations, fragments of spider silk peptides and different homopeptides consisting of up to $N = 22$ amino acids (aa) are pulled laterally over various polar and unpolar diamond surfaces in the presence of typically 3000 explicit water molecules. To do so, a harmonic spring is connected with one end to the peptide terminus, and the other end is moved parallel to the diamond surface at constant velocity V, as schematically shown in the inset of Figure 1A; from the average spring extension the average friction force is deduced. Surfaces with typical area 6 nm × 3 nm are designed and characterized by the fraction Φ of surface OH groups; we compare results for $\Phi = 0$, 11, 25, and 50%. In Figure 1A we show the friction force per aa, F_f/N, for a $N = 15$ spider silk fragment on unpolar $\Phi = 0\%$ (triangles) and polar $\Phi = 11\%$ (spheres) surfaces as a function of the pulling velocity V. For the unpolar surface, equilibration is not an issue:[22] The peptide chain glides smoothly over the surface (see SI), and the total friction force (solid triangles) grows linear with V, as denoted by the solid line. Thus the friction is in the viscous regime, and the friction coefficient per aa is given by $\gamma_0 = F_f/(NV) \simeq 10^{-12}$ kg/s, very close to the value in bulk water, as deduced from our simulations and from experiments (see SI). The corresponding hydrodynamic radius R_H, defined by the Stokes relation, $\gamma_0 = 6\pi\eta R_H$, is $R_H \simeq 0.1$ nm and thus of the order of the spatial extent of a single aa. Note that the surface friction on the unpolar surface is dominated by water friction, as follows by comparing the surface friction contribution F_f^{surf} (due to forces on the peptide from surface atoms, open triangles) and the total friction force F_f (which is the sum of all forces coming from surface *and* water atoms, full triangles). On the polar $\Phi = 11\%$ surface the behavior is completely different: For low velocities around $V \approx 0.1$ m/s, friction forces are more than 100-fold
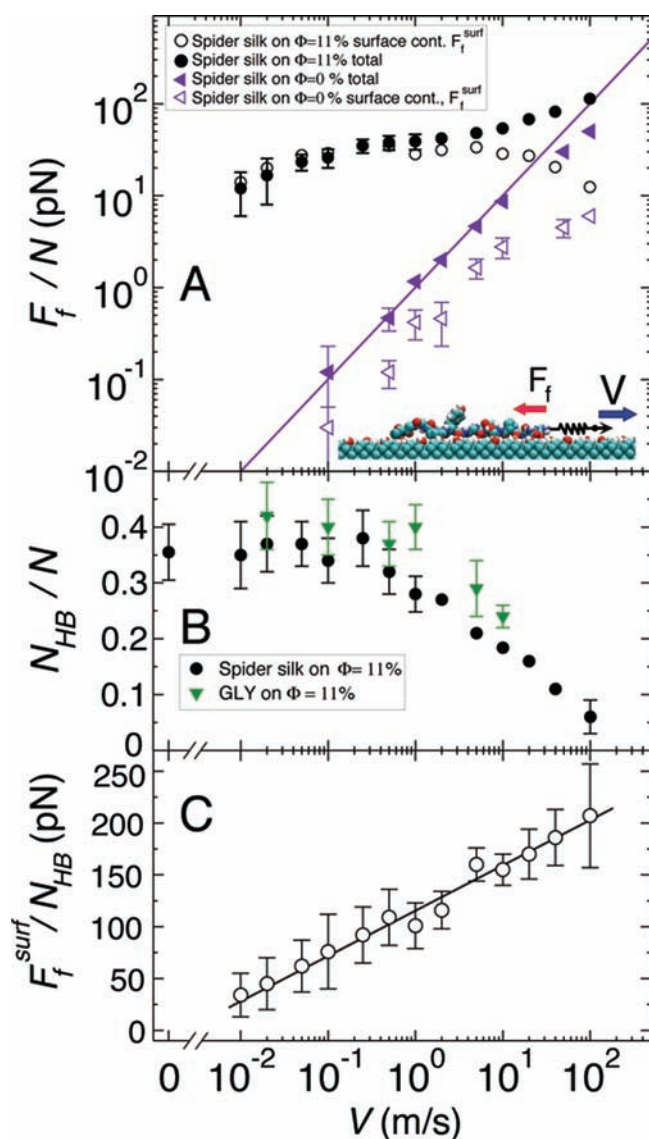
Figure 1. (A) Friction force per residue F_f/N versus pulling velocity V for $N = 15$ spider silk peptide on $\Phi = 11\%$ polar (solid spheres) and $\Phi = 0\%$ nonpolar diamond surfaces (solid triangles); open symbols denote the surface friction F_f^{surf}/N without the solvent contribution. Inset represents the simulation system. Straight line indicates the linear viscous law $F_f/N = \gamma_0 V$ with monomeric friction coefficient $\gamma_0 = 10^{-12}$ kg/s on the unpolar surface. (B) Number of surface peptide HBs per residue N_{HB}/N on $\Phi = 11\%$ polar surface for $N = 15$ spider silk and $N = 11$ polyglycine. (C) Surface friction force per HB, F_f^{surf}/N_{HB}, for spider silk on $\Phi = 11\%$ polar diamond. The straight line corresponds to eq 1.

higher compared to the unpolar surface, and the system is far from the viscous regime; in other words, F_f is not linearly proportional to V. For velocities $V < 10$ m/s the total friction (solid circles) is dominated by force contributions from the surface (open circles), whereas for higher velocities the relative importance of solvent friction increases and the total friction data on the two surfaces converge (solid circles and triangles). The surface friction contribution on the polar surface (open circles) in fact shows a maximum at a velocity of about $V \simeq 1$ m/s, a phenomenon known from adhesive friction between polymeric and soft interfaces and rationalized by the converse velocity dependencies of the number of adhesive contacts and the friction contribution per adhesive contact.[14,15] Indeed, in

Figure 1B we show the number of peptide-surface HBs per aa, N_{HB}/N, for the spider silk peptide (black circles). HBs are defined by the combined Luzar−Chandler angle and distance criterion.[31] The data indicate that for pulling velocities below $V \approx 1$ m/s, N_{HB} is not affected by the pulling and roughly $N_{HB}/N \simeq 0.35$, close to the equilibrium value obtained at $V = 0$ (included at the left in the graph). Indeed, for larger velocities, N_{HB} decreases, which is responsible for the maximum in F_f^{surf} in Figure 1A. The data for an $N = 11$ polyglycine chain, indicated by triangles, exhibit similar behavior but saturate at a slightly higher value of N_{HB}/N for low V due to the lack of bulky side chains; a detailed analysis of side chain and backbone HB distributions is presented below. Assuming a typical HB length scale $a_{HB} \simeq 0.1$ nm, a relaxation time τ_{HB} can be inferred from the crossover velocity seen in Figure 1B, $V_{HB} \simeq 1$ m/s, as $\tau_{HB} \approx a_{HB}/V_{HB} \simeq 100$ ps, a value that is somewhat larger than for HB relaxation in bulk water[31,32] but otherwise not implausible. One could therefore be led to think that for $V < V_{HB}$ simulations are in the linear regime where friction force is simply proportional to V. However, in Figure 1C, we demonstrate the surface friction force data from Figure 1A, rescaled by the number of HBs, to show perfect scaling,

$$F_f^{surf}/N_{HB} \simeq F_0 \ln(V/V_0) \qquad (1)$$

with $F_0 = 19.0$ pN and $V_0 = 0.0023$ m/s, over the whole velocity range probed in the simulations. A logarithmic velocity dependence of rupture and friction forces[4,14,15] is the signature of force-assisted thermal crossing of energetic barriers. The velocity scale V_0 is more than 2 orders of magnitude lower than the crossover velocity $V_{HB} \simeq 1$ m/s for the average HB population, which illustrates that there is a slow time scale that dominates the friction properties of HBs. Therefore, reaching the viscous regime, i.e., $V < V_0$, is a serious issue in biomolecular MD simulations:[5,7] To reach a distance of 2 nm at a pulling speed of V_0, the simulation time is 1 μs, which for large systems is a considerable task. At larger pulling speeds $V > V_0$, the pulling-force-induced changes of the free energy landscape produce nonlinear effects. In the simplest scaling-type derivation of eq 1, one writes the lifetime of an HB as $\tau \simeq \tau_0 e^{(U-a_0F)/k_BT}$, where U is the activation energy, F the externally applied force, τ_0 the intrinsic time scale, and a_0 a typical distance characterizing the barrier position. Denoting the velocity as $V \simeq a_0/\tau$, one obtains eq 1 with $F_0 = k_BT/a_0$ and $V_0 = (a_0/\tau_0) e^{-U/k_BT}$. With the fit value $F_0 = 19$ pN, we immediately obtain $a_0 = k_BT/F_0 \simeq 0.2$ nm on the order of the HB bond length (but note that the meaning of a_0 is actually more abstract and not necessarily of simple geometric nature, see below). Further setting $\tau_0 \approx a_0^2\gamma_0/k_BT$, i.e., associating the intrinsic time scale with the diffusion time over a typical distance a_0, and using for the intrinsic friction the value $\gamma_0 \simeq 10^{-12}$ kg/s valid for aa diffusion in bulk and at the hydrophobic surface, we conclude from the fit value for V_0 that $e^{U/k_BT} \approx 10^4$. Thus the energy scale is predicted to be of the order $U \simeq 10k_BT$, in considerable excess of the free energy of a single HB of the order of $2-3k_BT$,[33] which hints at strong cooperativity of HB friction, in accord with previous HB rupture studies.[6] In the linear force regime, $a_0F/k_BT < 1$, time scales are predicted to be slowed by a factor of $\tau/\tau_0 \approx e^{U/k_BT} \approx 10^4$ at the polar surface, including the viscous friction coefficient in the low velocity limit $V < V_0$, in rough agreement with the data in Figure 1A. Although $V_0 \simeq 0.002$ m/s is small for common MD simulations, it is orders of magnitude larger than typical

velocities in molecular biology or single-molecule experiments,[5−7,34] which are in the μm/s range. Since our main goal in this paper is the viscous friction of HBs in the linear regime $V \ll V_0$, we will later introduce a more general model that contains eq 1 as a special case and allows us to robustly extrapolate simulation data into the $V \ll V_0$ limit.

Effect of Normal Forces. In the macroscopic world, Amontons' law, $F_f = \mu F_N$, which states that the friction force is proportional to the normal force F_N and a constant μ of order unity, but in particular independent of sliding velocity and apparent contact area, very successfully describes friction in the absence of adhesion and for not too low sliding velocities.[13,14] In order to test the influence of normal forces on single-molecule friction, we apply an acceleration on each peptide atom inversely proportional to its mass, which amounts to a force that uniformly pushes the peptides onto the surface. Experimentally, normal forces have been realized in single-molecule studies by osmotic pressure techniques.[35] In Figure
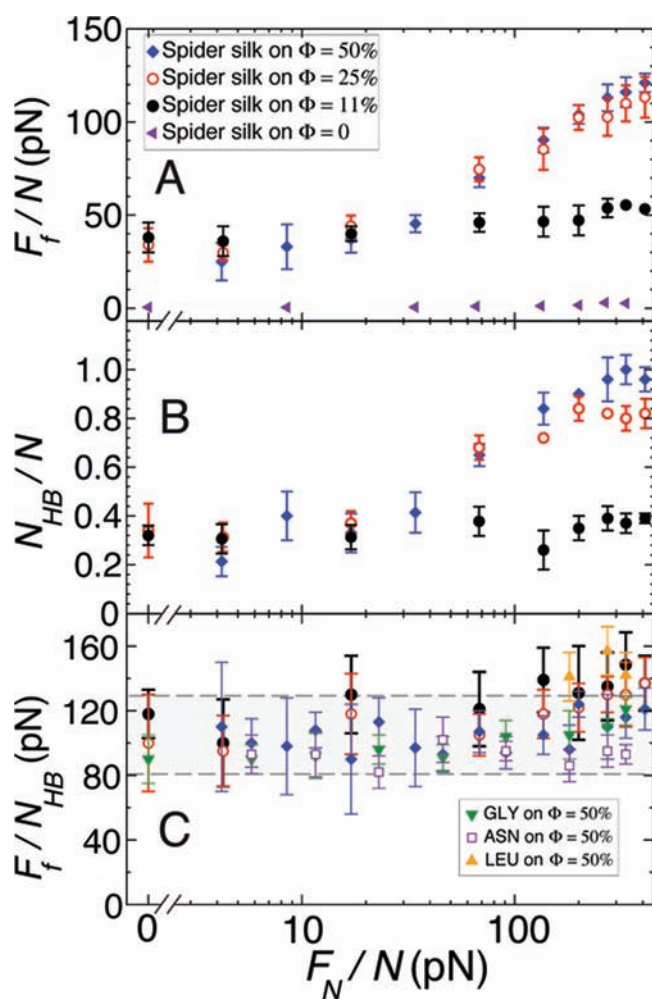
up to $F_N/N = 420$ pN for fixed pulling velocity $V = 0.5$ m/s. The higher F_N/N, the larger the friction force F_f/N, but the behavior differs from Amontons' law in that (i) friction saturates for large F_N/N and (ii) friction is nonzero for $F_N/N \rightarrow 0$. We also observe that F_f/N saturates as Φ increases, and that on the unpolar surface, $\Phi = 0\%$, friction is negligibly small even for large F_N. Figure 2B shows that the behavior of the HB number N_{HB} largely parallels the data in Figure 2A, which suggests that we should consider the friction force per HB, F_f/N_{HB}, which is plotted in Figure 2C. Here we add, in addition to the spider silk data in Figure 2A,B, data for polyglycine, polyasparagine, and polyleucine on a $\Phi = 50\%$ surface: the data for all peptides on different surfaces fall within a force range around $F_f/N_{HB} \simeq 100$ pN for the complete F_N/N range. This in turn means that the saturation behavior of the friction force for increasing Φ and increasing F_N in Figure 2A is explained by the limited HB formation capacity between peptide and surface, similar to recent findings for dry nanocontact friction.[36] This situation is schematically illustrated in Figure 3A: For increasing
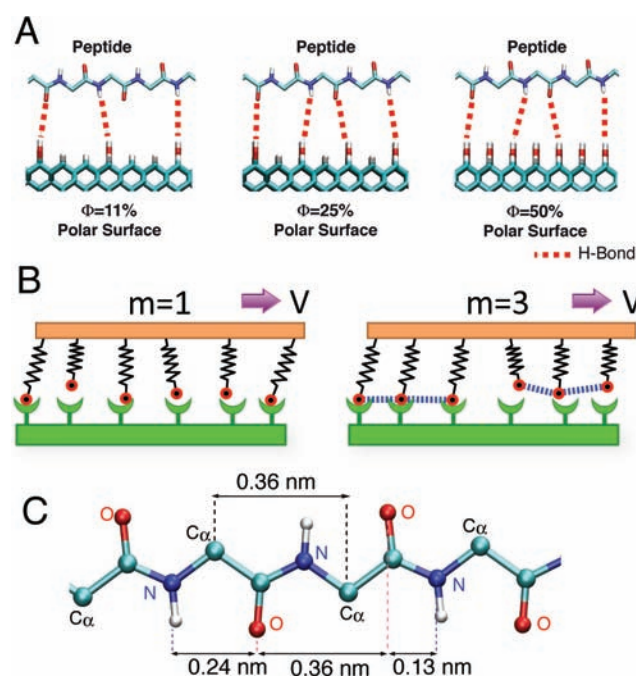

Figure 3. (A) Illustration of surface−peptide hydrogen-bonding for different surface OH fractions Φ. For small $\Phi = 11\%$ the number of HBs is limited by Φ; when all peptide groups are saturated, beyond $\Phi = 25\%$, a further increase of Φ does not increase N_{HB}. (B) In the absence of cooperativity, $m = 1$, HBs act independently; for finite cooperativity factor $m = 3$, three HBs break and re-form collectively. (C) Per residue there are two main HB contributors on the backbone: the oxygen and the hydrogen connected to the nitrogen. The average distance between HB-forming groups is 0.18 nm.

Φ, the number of HBs can only increase up to a point where all HB donors/acceptors on the peptide are engaged in bonding.

F_f/N and N_{HB}/N for polyglycine, polyasparagine, and polyleucine with $N = 11$ obtained on a $\Phi = 50\%$ OH-covered surface as a function of F_N/N for $V = 0.5$ m/s are shown in Figure 4A,B. As for the spider silk data, for normal forces below $F_N/N \simeq 90$ pN, the friction forces do not depend sensitively on the normal force, and the highest friction force is observed for polyglycine. This is because a polyglycine chain strongly adsorbs on the surface even for vanishing normal force. In
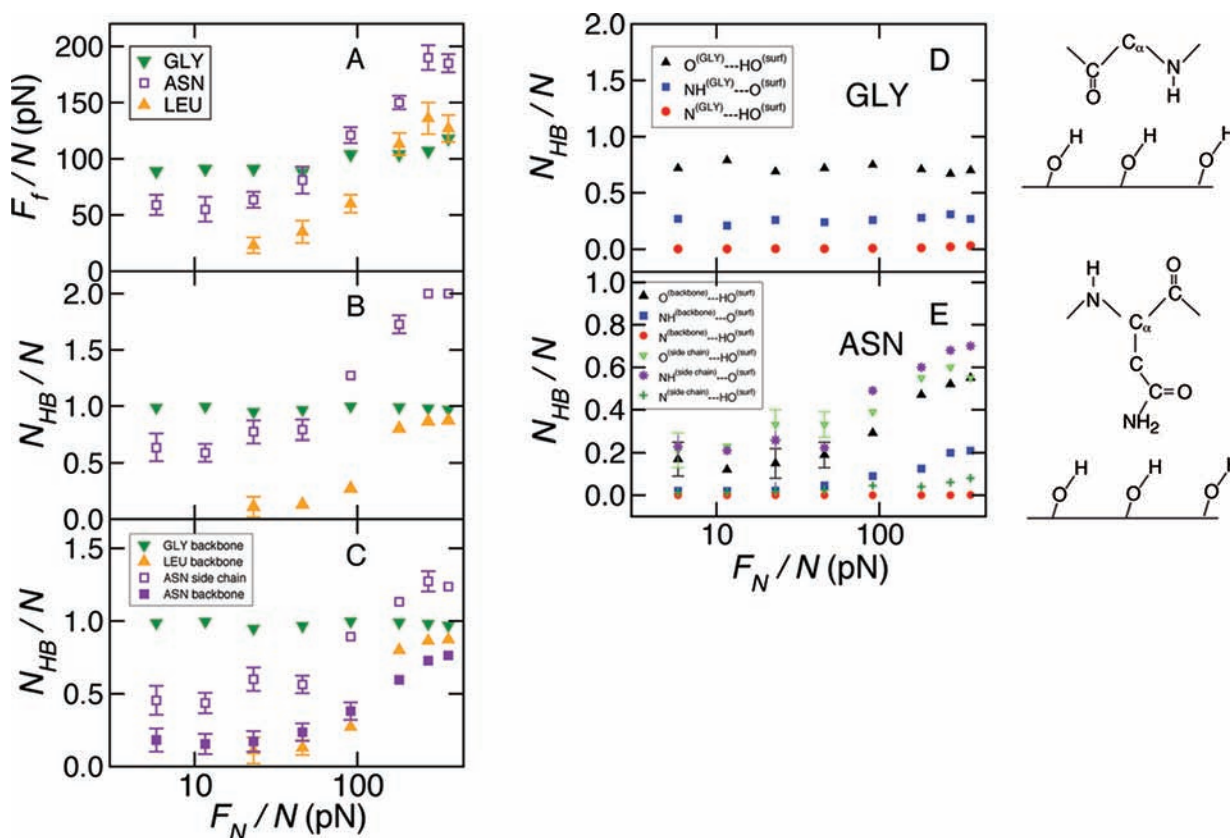

Figure 2. Effect of normal force: (A) friction force F_f/N, (B) number of surface−peptide HBs N_{HB}/N, and (C) friction force per HB F_f/N_{HB} versus normal force per residue F_N/N. Data are shown for $N = 15$ spider silk on $\Phi = 0$, 11, 25, and 50% OH-covered surfaces and in (C) also for $N = 11$ polyglycine, polyasparagine, and polyleucine for $\Phi = 50\%$. Pulling velocity is $V = 0.5$ m/s for all cases.

2A, the friction force per aa, F_f/N, obtained on surfaces with four different OH group concentrations, $\Phi = 0$, 11, 25, and 50%, is displayed as a function of normal force per aa ranging

Figure 4. Results for polyglycine, polyasparagine, and polyleucine homopeptide chains: (A) friction force, (B) surface–peptide HB number, (C) HB contributions from peptide side chains and the backbone, (D) HB contributions from all possible donor and acceptor combinations for $N = 11$ polyglycine, and (E) for $N = 11$ polyasparagin versus rescaled normal force. All data on the 50% OH-covered diamond and for fixed pulling velocity $V = 0.5$ m/s. Note that polyglycine and polyleucine have no polar side chain groups.

contrast, the strongly hydrophobic polyleucine chain desorbs from the surface for small normal forces, and this is why data are missing for polyleucine for small F_N/N. Note that the very hydrophilic polyasparagine also shows a smaller friction and a lower HB number than polyglycine, which shows that there is not a simple relation between the hydrophilicity of a peptide chain and the number of HBs it forms with a given surfaces.

Detailed Hydrogen Bond Number Analysis. We present a detailed analysis of backbone and side chain hydrogen-bonding and classify HBs according to acceptor/donor atoms. As shown in Figure 4A, at $F_N \simeq 90$ pN, the friction force for polyasparagine becomes larger than that for polyglycine. This crossover in fact can be associated with the increasing contribution of asparagine side chain HBs with increasing normal force, as illustrated in Figure 4C. The number of HBs from the asparagine backbone also increases with rising normal force but always stays below the backbone contribution obtained with glycine. For the entire normal force range, the polar side chains of polyasparagine form more HBs with the surface than the backbone. Although all three polypeptides have identical backbones, the polyglycine backbone is most efficient in forming HBs with the surface. For polyleucine, this is easily understood, since the large unpolar polyleucine side chains block the polar backbone groups from forming HBs. Increasing normal force pushes the polyleucine backbone toward the surface, and the backbone polar groups finally form HBs with the surface for normal forces $F_N \geq 90$ pN, as shown in Figure 4C. For polyasparagine we propose a subtle competition between side-chain and backbone HBs that

might explain why the backbone forms fewer HBs than polyglycine, as appreciated from Figure 4C.

In the geometrical definition of an HB, the atom which is covalently bonded to the H atom is called the donor, and the third atom is termed acceptor. On the peptide and on the surface, we have various donors and acceptors for HB formation: On the peptide backbone, both O and N atoms can operate as acceptor. The same N atoms can also act as a donor via the NH group. On the surface, the O atom can both be an acceptor and a donor. This means that the backbone (i.e., glycine) can form three different types of HBs: NH⋯O, O⋯HO, and N⋯HO. In Figure 4D, we show all of these HBs for an $N = 11$ polyglycine chain as a function of the applied normal force. It turns out that the main contribution to N_{HB} is due to two types of HBs: NH⋯O and O⋯HO. The N atom contributes negligibly as an acceptor to N_{HB}, as shown in Figure 4D. In Figure 4E, we show the results of a similar analysis also for $N = 11$ polyasparagine. Similar to polyglycine, N⋯HO-type HBs have negligible weight in N_{HB}.

Stochastic Model for Hydrogen Bond Friction. Stimulated by the scaling displayed in Figure 2C, we introduce a simple stochastic model that describes the full velocity dependence of the friction per HB and allows robust extrapolation of simulation data into the relevant viscous regime for $V < V_0$. Our model is motivated by three observations: (i) Although the scaling law in eq 1 allows us to hand-wavingly extract the viscous friction coefficient via the time scale ratio τ/τ_0, as outlined above, it does not describe the crossover from logarithmic to linear friction around $V \simeq V_0$. (ii)

The more general Schallamach model[14,15] yields this crossover but contains a handful of fit parameters which cannot be robustly extracted from the limited data shown in Figure 1A. (iii) Since the viscous regime (for $V < V_0$) occurs much below the crossover V_{HB} (above which N_{HB} depends on V), we can safely use N_{HB}^{eq}, i.e., the equilibrium value of N_{HB} for $V < V_{HB}$, in order to extract the linear friction coefficient. We thus define the friction coefficient per HB as

$$\gamma_{HB} \equiv F_f/(V N_{HB}^{eq}) \tag{2}$$

which is shown in Figure 5 as a function of the rescaled friction force F_f/N for polyglycine (A) and spider silk (B). In this plot,
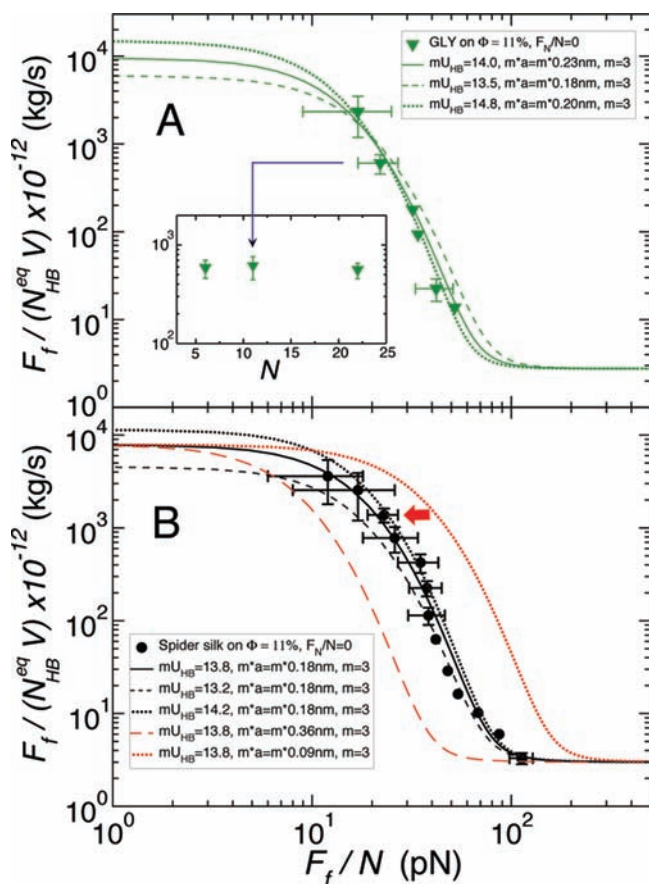

Figure 5. Comparison of the simulation data for the friction coefficient per equilibrium HB number, $\gamma_{HB} = F_f/(V N_{HB}^{eq})$, with the Fokker−Planck solution given in eq 3 as function of F_f/N: (A) $N = 11$ polyglycine for $\Phi = 11\%$ with $N_{HB}^{eq} = 4$; (B) $N = 15$ spider silk for $\Phi = 11\%$, $N_{HB}^{eq} = 5$. The data marked by the red arrow are studied in more detail in Figure 6. The inset of (A) shows γ_{HB} versus N for polyglycine and $\Phi = 11\%$ for fixed pulling velocity $V = 0.1$ m/s.

one discerns the onset of saturation of γ_{HB} for low F_f/N, in particular for the spider silk data in Figure 5B, but in order to reliably extrapolate the data to $F_f/N \rightarrow 0$ (and thus to $V \ll V_0$) one needs a theory that encompasses both nonlinear and linear friction regimes. Adopting an early model for the hindered diffusion of a protein along its one-dimensional folding reaction coordinate,[11,37] we consider a single particle in a sinusoidal potential of periodicity a, $U(x) = m U_{HB}(\cos[2\pi x/a] - 1)/2$, where U_{HB} denotes the HB free energy and the cooperativity factor m measures how many HBs break collectively, as depicted schematically in Figure 3B. The friction coefficient can

be written as

$$\gamma_{HB} = \frac{N\gamma_0}{N_{HB}^{eq}} + \frac{\gamma_0}{m}\Psi\left(\frac{maF_f}{k_B T N_{HB}^{eq}}, \frac{m U_{HB}}{k_B T}\right) \tag{3}$$

where the first term is due to solvent friction and γ_0 is the solvent friction coefficient, which is taken as $\gamma_0 = 10^{-12}$ kg/s. The function Ψ describes the friction of one cooperative unit consisting of m HBs, driven by the force $m F_f/N_{HB}^{eq}$ in the potential $U(x)$, which follows from the closed-form solution of the Fokker−Planck equation[11] (see SI for details and the connection to eq 1). Note that we assume the total friction force F_f to be equally shared by all N_{HB} HBs; the force acting on one HB is thus F_f/N_{HB}^{eq} and the force acting on one cooperative unit consisting of m HBs follows as $m F_f/N_{HB}^{eq}$. In Figure 5B, eq 3 fits spider silk data quite accurately for $m U_{HB} = 13.8 k_B T$, $a = 0.18$ nm, and $m = 3$ (solid black line); for polyglycine in Figure 5A the fit yields slightly adjusted parameters (green solid line). These numbers roughly agree with the scaling-type interpretation of the fit in Figure 1C. The dotted and broken black/green lines denote equally acceptable fits and thus allow us to estimate the error in the fit values. The red lines demonstrate that the periodicity a corresponds to a shift along the F_f/N axis and can be determined with high accuracy. Extrapolation to the limit of $F_f \rightarrow 0$ gives only slightly different values for γ_{HB} for the two peptides, so we conclude that the viscous friction coefficient per HB is quite generally given by $\gamma_{HB} \simeq 10^{-8}$ kg/s. Due to the exponential dependence on $m U_{HB}$ in the double limit $m U_{HB}/k_B T \gg 1$ and $m a F_f/k_B T N_{HB}^{eq} \rightarrow 0$, $\Psi \simeq e^{m U_{HB}/k_B T}/(\pi m U_{HB}/k_B T)$, apart from the combination $m U_{HB}$, the cooperativity factor by itself, m, is subfluent and influences the functional form of Ψ only mildly (see SI). The factor m is introduced mainly to reconcile the surprisingly high fit value of $m U_{HB}$ with the known (considerably smaller) HB free energy[33] and suggests that m HBs break and form cooperatively upon diffusion of the peptide. It is *a priori* not clear whether the activation energy U_{HB} is given by the HB free energy in vacuum, easily reaching $10 k_B T$, or by the HB free energy in water, more of the order of $2-3 k_B T$,[33] since HB donors and acceptors are shielded from ambient water by the presence of the peptide on the surface. Assuming an HB activation free energy of $U_{HB} \simeq 5 k_B T$, we arrive at a cooperativity factor $m = 3$, close to what has been seen in force-induced breakage of HB assemblies.[6] Assuming a different value for U_{HB} would result in a modified value for m without changing the quality of the fit or the conclusion of our paper, as demonstrated in detail in the SI.

To show that finite-size effects are not important and in particular that the cooperativity is not set by the system size, we show in the inset of Figure 5A γ_{HB} for polyglycine of varying size $N = 6$, 11, and 22 at fixed pulling velocity $V = 0.1$ m/s. The friction coefficient per HB is roughly constant and independent of peptide length, which shows that HB friction is extensive and scales proportional with the peptide length and thus HB number. It is the extensive scaling property of the friction force together with the large friction coefficient per HB that suggests the existence of cooperative units of m HBs that act collectively.

The distance between two OH groups on the $\Phi = 11\%$ polar surface is roughly 1 nm. We recall that only two groups on the backbone are able to form HBs in appreciable quantity, and the average distance between these groups along the backbone is roughly 0.18 nm. In fact, the fit result for the periodicity length scale, $a \simeq 0.18$ nm, turns out to match the distance between HB forming groups on a peptide chain, as schematically illustrated
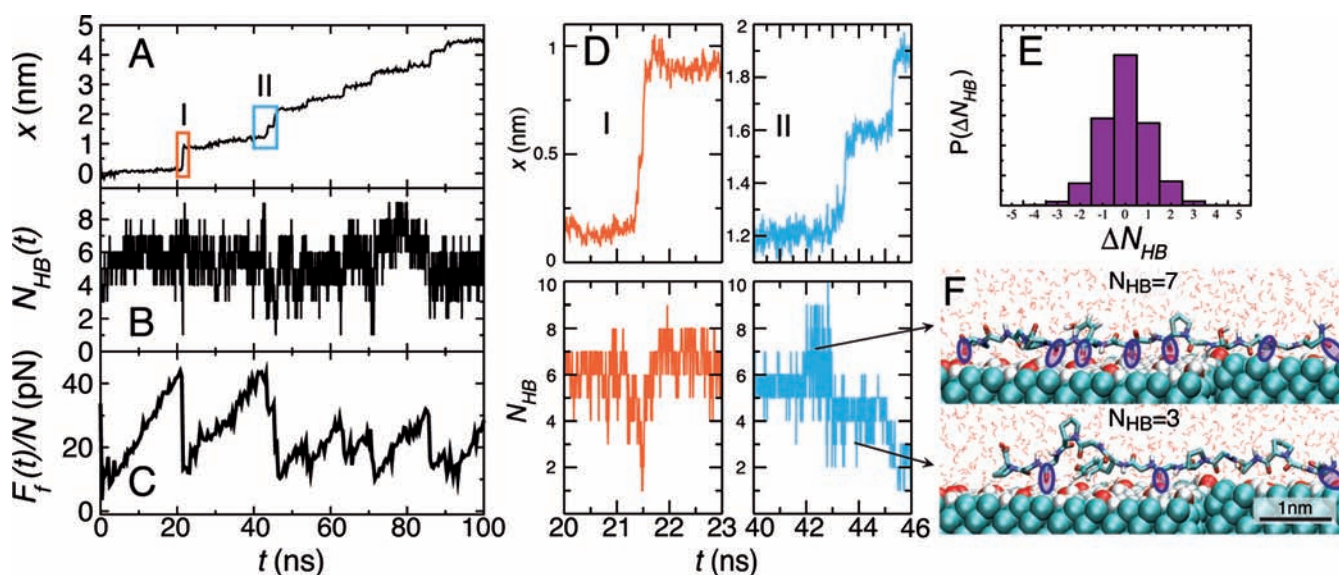
Figure 6. Simulation trajectory analysis for $N = 15$ spider silk on $\Phi = 11\%$ polar surface for pulling velocity $V = 0.05$ m/s: (A) Displacement of the terminal residue, (B) surface−peptide HB number N_{HB}, and (C) friction force as a function of time. (D) High-resolution trajectories for the two colored boxes indicated in (A). (E) HB number change distribution $\Delta N_{HB} = N_{HB}(t + \Delta t) - N_{HB}(t)$ for time step $\Delta t = 8$ ps. (F) Peptide snapshots at two different times in the trajectory in (D). Surface−peptide HBs are marked by ellipses.

in Figure 3C. This findings suggests that when two HB forming surfaces slide against each other, the one with the smaller periodicity will set the effective periodicity a. Note that the two possible HBs the backbone of an aa can form, for geometric reasons are typically not present simultaneously. Indeed, the average number of HBs per aa is typically much lower than unity, as shown in Figure 2. Nevertheless, the velocity dependent friction force seems to reflect the minimal possible distance between HB forming groups on the peptide via the stochastic and cooperative forming and breaking of HBs.

The cooperative friction manifests itself as stick−slip behavior with collective HB breaking events, as shown in Figure 6, where one typical spider silk trajectory on a $\Phi = 11\%$ polar surface is depicted (see SI for analogous polyglycine data). Figure 6A shows time traces of the displacement of the pulled terminal aa, Figure 6B the instantaneous number of HBs, N_{HB}, and Figure 6C the friction force per aa, F_f/N. Slip events in the displacement x correlate with sudden decreases in F_f/N and, as shown more clearly in the zoomed trajectories in Figure 6D, with drops in the HB number, quite similar to stick−slip phenomena in boundary lubrication.[38] In Figure 6F two snapshots of the peptide before and after a slip event are shown, surface−peptide HBs are marked by ellipses. In fact, the distribution of HB number changes, $\Delta N_{HB} = N_{HB}(t + \Delta t) - N_{HB}(t)$ at a fixed time frame of $\Delta t = 8$ ps, shown in Figure 6E, is rather narrow. This suggests that slip-producing HB breaking events, associated with $\Delta N_{HB} \pm 3$ according to our friction analysis, make up only a small fraction of all HB breaking events.

■ CONCLUSION

On the basis of solvent-explicit MD simulations for a peptide sliding over polar surfaces, performed for a wide range of pulling velocities from $V = 0.01$ to 100 m/s, we have established the friction law for hydrogen-bonded matter and in particular showed that the friction force is proportional to the number of HBs both in the viscous friction regime (where

friction is proportional to sliding velocity) and in the nonlinear regime for $V > V_0 \simeq 0.002$ m/s.

The viscous friction coefficient per HB turns out to be $\gamma_{HB} \approx 10^{-8}$ kg/s and thus amounts to the Stokes friction of a sphere with an equivalent radius of roughly 1 μm moving in water. This means that at a biologically relevant velocity of $V \approx 1$ μm/s, the friction force of a single HB is only $F_f \approx 10^{-14}$ N, so that the combined action of 100 HBs would be necessary to raise the force to 1 pN. The time for an assembly of N_{HB} HBs to diffuse over a length corresponding to the contour aN_{HB} is given by $\tau \simeq N_{HB}^3 a^2 \gamma_{HB}/(k_B T)$. Taking $a = 0.2$ nm and $\gamma_{HB} \simeq 10^{-8}$ kg/s we obtain $\tau \simeq N_{HB}^3 \times 100$ ns, thus for $N_{HB} = 5$ we obtain a diffusional time in the order of 10 μs (note that our friction law is not valid for a single HB but only for N_{HB} beyond the cooperativity scale m). This finding is interesting in light of a puzzle in protein folding: while the typical times for the folding of structural motifs such as a 21-residue α helix[39] and the contact formation for 10-residue unstructured proteins[9,10] are in the 10−100 ns range, protein folding times are typically much larger.[40] As shown above, HB friction associated with the iso-free-energetic diffusive escape from misfolded motifs can easily account for diffusional times in the microsecond scale.

We finally note that for assemblies larger than the cooperativity scale, HB friction should probably not be visualized as roughness in a 1D free energy landscape, rather, for proteins it is one contribution to internal friction in a diffusional protein folding picture.[12] HB friction will be most pronounced in β strands and other filamentous structures, since an initial misalignment will have to heal by diffusion. This might explain recent experiments on three-helix-bundle proteins, where mutations cause large changes in folding kinetics without major modifications in the free energy landscape.[41]

An important factor determining the friction coefficient turns out to be the cooperativity factor m, since it appears exponentially.[42] For two rather stiff surfaces that can hydrogen-bond, the cooperativity will be higher than when the scaffolding matrices are very loose and flexible. In that sense,

the setup chosen by us, one peptide on a stiff surface, besides being efficient from the simulation point of view, constitutes an intermediate case.

■ ASSOCIATED CONTENT

ⓢ Supporting Information

Further discussion about friction in bulk water and on the unpolar surface, stochastic model for HB friction, stick−slip behavior, cooperativity in MD simulations, and simulation details. This material is available free of charge via the Internet at http://pubs.acs.org.

■ AUTHOR INFORMATION

Corresponding Author
rnetz@physik.fu-berlin.de

■ ACKNOWLEDGMENTS

■ REFERENCES

(1) Cordier, P.; Tournilhac, F.; Soulié-Ziakovic, C.; Leibler, L. *Nature* **2008**, *451*, 977.

(2) Sijbesma, R. P.; Beijer, F. H.; Brunsveld, L.; Folmer, B. J. B.; Hirschberg, J. H. K.; Lange, R. F. M.; Lowe, J. K. L.; Meijer, E. W. *Science* **1997**, *278*, 1601.

(3) Kushner, A. M.; Vossler, J. D.; Williams, G. A.; Guan, Z. *J. Am. Chem. Soc.* **2009**, *131*, 8766.

(4) Evans, E. *Annu. Rev. Biophys. Biomed.* **2001**, *30*, 105.

(5) Sotomayor, M.; Schulten, K. *Science* **2007**, *316*, 1144.

(6) Keten, S.; Buehler, M. J. *Nano Lett.* **2008**, *8*, 743.

(7) Kappel, C.; Grubmüller, H. *Biophys. J.* **2104**, *100*, 1109.

(8) Seifert, U. *Phys. Rev. Lett.* **2000**, *84*, 2750.

(9) Lapidus, L. J.; Eaton, W. A.; Hofrichter, J. *Proc. Natl. Acad. Sci. U.S.A.* **2000**, *97*, 7220.

(10) Moeglich, A.; Joder, K.; Kiefhaber, T. *Proc. Natl. Acad. Sci. U.S.A.* **2006**, *103*, 12394.

(11) Zwanzig, R. *Proc. Natl. Acad. Sci. U.S.A.* **1988**, *85*, 2029.

(12) Bryngelson, J. D.; Wolynes, P. G. *J. Phys. Chem.* **1989**, *93*, 6902.

(13) Gao, J.; Luedtke, W. D.; Gourdon, D.; Ruths, M.; Israelachvili, J. N.; Landman, U. *J. Phys. Chem. B* **2004**, *108*, 3410−3425.

(14) Baumberger, T.; Caroli, C. *Adv. Phys.* **2006**, *55*, 279.

(15) Drummond, C.; Israelachvili, J.; Richetti, P. *Phys. Rev. E* **2003**, *67*, 066110.

(16) Maier, B.; Rädler, J. O. *Phys. Rev. Lett.* **1999**, *82*, 1911.

(17) Pastré, D.; Piétrement, O.; Zozime, A.; Cam, E. L. *Biopolymers* **2004**, *77*, 53.

(18) Kühner, F.; Erdmann, M.; Sonnenberg, L.; Serr, A.; Morfill, J.; Gaub, H. E. *Langmuir* **2006**, *22*, 11180.

(19) Kuehner, F.; Morfill, J.; Neher, R. A.; Blank, K.; Gaub, H. E. *Biophys. J.* **2007**, *92*, 2491.

(20) Bormuth, V.; Varga, V.; Howard, J.; Schaffer, E. *Science* **2009**, *325*, 870.

(21) Horinek, D.; Serr, A.; Geisler, M.; Pirzer, T.; Slotta, U.; Lud, S. Q.; Garrido, J. A.; Scheibel, T.; Hugel, T.; Netz, R. R. *Proc. Natl. Acad. Sci. U.S.A.* **2008**, *105*, 2842.

(22) Serr, A.; Horinek, D.; Netz, R. R. *J. Am. Chem. Soc.* **2008**, *134*, 235102.

(23) Wiemers, K.; Kauffman, J. F. *J. Phys. Chem. A* **2000**, *104*, 451.

(24) Dickrell, P. L.; Pal, S. K.; Bourne, G. R.; Muratore, C.; Voevodin, A. A.; Ajayan, P. M.; Schadler, L. S.; Sawyer, W. G. *Tribol. Lett.* **2006**, *24*, 85.

(25) Chen, J.; Ratera, I.; Park, J. Y.; Salmeron, M. *Phys. Rev. Lett.* **2006**, *96*, 236102.

(26) Lindahl, E.; Hess, B.; van der Spoel, D. *J. Mol. Model.* **2001**, *7*, 306.

(27) Scott, W. R. P.; Hünenberger, P. H.; Tironi, I. G.; Mark, A. E.; Billeter, S. R.; Fennen, J.; Torda, A. E.; Huber, T.; Krüger, P.; van Gunsteren, W. F. *J. Phys. Chem. A* **1999**, *103*, 3596.

(28) Berendsen, H. J. S.; Postma, J. P. M.; van Gunsteren, W. F.; Hermans, J. *Intermolecular Forces* **1981**, 331.

(29) Feenstra, K. A.; Hess, B.; Berendsen, H. J. S. *J. Comput. Chem.* **1999**, *20*, 786.

(30) Darden, T.; York, D.; Pedersen, L. *J. Chem. Phys.* **1993**, *98*, 10089.

(31) Luzar, A.; Chandler, D. *Nature* **1996**, *379*, 55.

(32) von Hansen, Y.; Sedlmeier, F.; Hinczewski, M.; Netz, R. R. *Phys. Rev. E* **2011**, *84*, 051501.

(33) Fersht, A. R.; Shi, J. P.; Knill-Jones, J.; Lowe, D. M.; Wilkinson, A. J.; Blow, D. M.; Brick, P.; Carter, P.; Waye, M. M. Y.; Winter, G. *Nature* **1985**, *314*, 235.

(34) Li, Q.; Dong, Y.; Perez, D.; Martini, A.; Carpick, R. W. *Phys. Rev. Lett.* **2011**, *106*, 126101.

(35) Lau, A. W. C.; Prasad, A.; Dogic, Z. *EPL (Eur. Phys. Lett.)* **2009**, *87*, 48006.

(36) Mo, Y.; Turner, K. T.; Szlufarska, I. *Nature* **2009**, *457*, 1116.

(37) Ruckenstein, E.; Tsekov, R. *J. Chem. Phys.* **1994**, *100*, 7696.

(38) Thompson, P. A.; Robbins, M. O. *Science* **1990**, *250*, 792.

(39) Williams, S.; Causgrove, T. P.; Gilmanshin, R.; Fang, K. S.; Callender, R. H.; Woodruff, W. H.; Dyer, R. B. *Biochemistry* **1996**, *35*, 691.

(40) Yang, W. Y.; Gruebele, M. *Nature* **2003**, *423*, 193−197.

(41) Wensley, B. G.; Batey, S.; Bone, F. A. C.; Chan, Z. M.; Tumelty, N. R.; Steward, A.; Kwa, L. G.; Borgia, A.; Clarke, J. *Nature* **2010**, *463*, 685.

(42) Müser, M. H.; Robbins, M. O. *Phys. Rev. B* **2000**, *61*, 2335.